Langmuir

Article

pubs.acs.org/Langmuir

Multistep Galvanic Exchange Synthesis Yielding Fully Reduced Pt Dendrimer-Encapsulated Nanoparticles

Rachel M. Anderson, David F. Yancey, James A. Loussaert, and Richard M. Crooks*

Department of Chemistry and Texas Materials Institute, The University of Texas at Austin, 105 East 24th Street, Stop A5300, Austin, Texas 78712-1224, United States

Supporting Information

ABSTRACT: Here we outline a new method for synthesizing fully reduced Pt dendrimer-encapsulated nanoparticles (DENs). This is achieved by first synthesizing Cu DENs of the appropriate size through sequential dendrimer loading and reduction steps, and then galvanically exchanging the zerovalent Cu DENs for Pt. The properties of Pt DENs having an average of 55, 140, and 225 atoms prepared by direct chemical reduction and by galvanic exchange are compared. Data obtained by UV−vis spectroscopy, X-ray absorption spectroscopy, X-ray photoelectron spectroscopy, and high-resolution electron microscopy confirm only the presence of fully reduced Pt DENs when synthesized by galvanic exchange, while chemical reduction leads to a mixture of reduced DENs and unreduced precursor. These results are significant because Pt DENs are good models for developing a better understanding of the effects of finite size on catalytic reactions. Until now, however, the results of such studies have been complicated by a heterogeneous mixture of Pt catalysts.

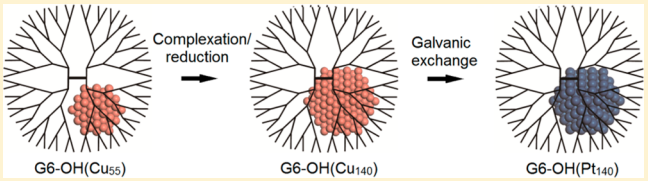

INTRODUCTION

Dendrimer-encapsulated nanoparticles (DENs) are well-defined nanoparticles having sizes ranging from just a few atoms[1] to perhaps 300 atoms.[2,3] This is the most scientifically interesting range of metal particle sizes because the addition of just a few atoms can drastically change their optical, electrical, mechanical, and catalytic properties.[4−7] For fundamental studies of catalytic properties, DENs are particularly useful for two reasons. First, it is possible to control their size, composition, and structure over a fairly broad parameter space, which is important for comparing theoretical calculations with experimental data.[8−10] Second, the presence of the dendrimer protects the particles from agglomeration without poisoning the metal surface. For both of these reasons, DENs are one of the best model materials available for studying the fundamental properties of electrocatalytic reactions on metal particles in the 1−2 nm size range.

Pt is one of the most important catalytic metals, and hence Pt DENs have been studied as catalysts for homogeneous,[11,12] heterogeneous,[13] and electrocatalytic[14−16] reactions. However, we[17] and others[18−21] have previously pointed out that correlations between theory and experiment with DENs are complicated by incomplete reduction of the Pt salt used as the nanoparticle precursor. This situation is unique to Pt DENs and is a consequence of the method used to prepare them. Pt DENs, and DENs in general, are usually synthesized in two steps.[2,3] First, the poly(amidoamine) (PAMAM) dendrimer and precursor metal salt are mixed together, and this results in encapsulation of the precursor within the dendrimer interior. Second, a strong reducing agent like BH_4^- is added to the resulting solution. This leads to reduction of the precursor and subsequent intradendrimer agglomeration of the resulting atoms to yield the final nanoparticle.

For most metals, the addition of BH_4^- results in complete reduction of the precursor metal salt. Pt is unusual, however, in that the synthesis leads to a bimodal distribution of fully reduced DENs and fully unreduced, Pt^{2+}-containing dendrimers.[17] We explained this observation by invoking a nucleation and growth mechanism for Pt DENs. Within this framework, zerovalent Pt seeds form in some dendrimers but not in others. In the presence of seeds, additional reduction of Pt^{2+} within that dendrimer is autocatalytic. However, if no seed forms, then the metal salt is kinetically trapped in its oxidized form. At this point we do not know with certainty why seeds form in some dendrimers and not in others, but the problem has been studied by others.[18−20,22] For example, Borodko et al.[19] reported that multidentate binding of Pt^{n+} to amine groups within the dendrimer hinders the reduction of the precursor complex to zerovalent particles, presumably by shifting the redox potential of Pt^{n+} to more negative potentials. Subsequently, this same group showed that UV irradiation of the precursor can yield linear Pt chains containing 2−8 atoms, and that these seeds lead to the formation of nanocrystals.[20]

We have shown that small (~1.5 nm), fully reduced Pt DENs can be prepared using the method of galvanic exchange.[23] These materials are prepared by synthesizing Cu DENs using the usual BH_4^- reduction method, and then a Pt salt, such as $PtCl_4^{2-}$, is added to the solution. Because of their relative

Received: October 6, 2014
Revised: November 18, 2014
Published: December 2, 2014

reduction potentials, the Cu DENs are oxidized to Cu^{2+}, and the Pt salt is reduced to zerovalent Pt.[24] Although this method is highly effective, the largest Pt DENs that can be formed in sixth-generation PAMAM dendrimers by galvanic exchange contain just 64 atoms. This is a consequence of the fact that the maximum number of Cu^{2+} ions that can be sequestered within the dendrimer is 64 and that the Cu:Pt galvanic exchange stoichiometry is 1:1.[25] Clearly, it would be advantageous to use this same approach to prepare larger Pt DENs so that a broader size range of materials could be reliably synthesized.

In the present report, we use more advanced characterization tools, primarily scanning transmission electron microscopy (STEM) and X-ray absorption near edge structure (XANES) spectroscopy, to confirm that the standard BH_4^--reduction method leads to a bimodal distribution of reduced and unreduced Pt-dendrimer composite materials. More importantly, however, we describe a galvanic exchange-based synthetic procedure that leads to larger, fully reduced Pt DENs. The synthetic approach involves two steps. First, Cu DENs containing more than 64 atoms are prepared by carrying out multiple sequential complexation/reduction steps. Second, galvanic exchange of these larger Cu DENs with Pt^{2+} results in Pt DENs containing up to at least 225 atoms. We confirm that full reduction of Pt has occurred using UV−vis spectroscopy, X-ray photoelectron spectroscopy (XPS), and extended X-ray absorption fine structure (EXAFS) spectroscopy. This advance in the synthesis of model Pt DENs will allow for more accurate comparison of experimental properties to theory, which is the goal of our research in this field.

EXPERIMENTAL SECTION

Chemicals. Sixth-generation, hydroxyl-terminated (G6-OH) poly(amidoamine) (PAMAM) dendrimers in methanol were purchased from Dendritech (Midland, MI). Before use, the dendrimer solution was dried under vacuum and reconstituted in water at a concentration of 100.0 μM. Isopropyl alcohol and $NaBH_4$ were purchased from Sigma-Aldrich, K_2PtCl_4 was from Acros Organics, $CuSO_4$ and NaOH from Fisher Scientific, high-purity $HClO_4$ from J.T. Baker, and Vulcan carbon was from ElectroChem, Inc. (Woburn, MA). All solutions were made using deionized water having a resistivity of 18.2 MΩ·cm (Milli-Q gradient system, Millipore).

Synthesis of Pt DENs by BH_4^- Reduction. The Pt-dendrimer precursor complexes (G6-OH$(Pt^{2+})_n$, n = 55, 140, or 225) were prepared by allowing the appropriate amount (55, 140, or 225 equiv, respectively) of K_2PtCl_4 to complex with the interior of G6-OH (2.0 μM) for 72 h. The G6-OH$(Pt^{2+})_n$ precursor was reduced by adding 50 equiv of $NaBH_4$, and then tightly sealing the container for 24 h. To avoid high H_2 pressures, 15 mL samples of DENs were reduced in 20 mL vials. Note that in the past we have typically used a $NaBH_4$:Pt^{2+} ratio of 10:1, but it was increased here to facilitate maximum Pt^{2+} reduction. UV−vis spectra were acquired using a Hewlett-Packard HP8453 spectrometer. A 2.0 mm quartz cuvette was used and blanked with 2.0 μM G6-OH.

Synthesis of Pt DENs by Galvanic Exchange. The first step of the Pt DEN galvanic exchange synthesis is preparation of 55-atom Cu DENs using a previously reported procedure.[23−25] Briefly, a 2.0 μM solution of G6-OH PAMAM dendrimer was prepared from a 100.0 μM stock solution. To this, 55 equiv of $CuSO_4$ were added from a 0.010 M stock solution. Aliquots of 0.30 M NaOH were added to adjust the pH to ∼7.5, and this solution was stirred for 15 min to allow for Cu^{2+} complexation to the dendrimer. At this point, the solution was purged with N_2, and it was kept under N_2 for the remainder of the synthetic procedure. Next, an equivalent (molar) amount of $NaBH_4$ was added from a freshly made 0.10 M stock solution. Reduction was allowed to proceed for at least 5 min.

Once reduction was complete, excess unreacted BH_4^- was oxidized by adding a 4-fold excess (relative to the equiv of BH_4^-) of 0.1 M $HClO_4$ and allowing it to react for 5 min (the pH was maintained above 5 with NaOH throughout the synthesis). The pH of the solution was then raised to ∼6.5 so that additional equiv of Cu^{2+} could be complexed with the dendrimer. This cycle (adjust pH to >6.5, add Cu^{2+}, wait for complexation, reduce, oxidize excess BH_4^-) was repeated as many times as necessary to synthesize Cu DENs of the desired size. At this stage, the pH was lowered to 3.2 and galvanic exchange for Pt was carried out by adding sufficient Pt^{2+} (from a freshly prepared 0.10 M stock solution of $PtCl_4^{2-}$) to the Cu DENs solution so that the Pt^{2+}:Cu ratio was 1. The resulting Pt DENs solution was immediately immobilized on Vulcan carbon using the procedures described in the next two sections.

Analysis by Scanning Transmission Electron Microscopy (STEM). The G6-OH$(Pt^{2+})_n$ precursor, Pt DENs synthesized by chemical reduction, and Pt DENs synthesized by galvanic exchange (collectively referred to as Pt-dendrimer composites) were immobilized on Vulcan carbon by diluting a 2.0 μM solution of the Pt-dendrimer composite to 200 nM and then adding 2.0 mg of Vulcan carbon per mL of diluted Pt-dendrimer composite. This ratio of dendrimers:carbon ensured sufficient separation (for imaging purposes) between individual Pt-dendrimer composites on the surface of the Vulcan carbon. Isopropyl alcohol (final concentration: 20 vol %) was added to each solution to assist with dispersion of the carbon. The resulting ink was sonicated for 1 min, then 2.0 μL of this solution was pipetted onto a lacey-carbon-over-Ni transmission electron microscopy (TEM) grid (Electron Microscopy Sciences, Hatfield, PA), and finally the grid was dried in air. A JEOL JEM-ARM200F STEM with spherical aberration (Cs) correction and a high-angle annular dark-field (HAADF) detector was used for sample analysis.

Analysis by X-ray Absorption Spectroscopy (XAS). As for the STEM analysis, the Pt-dendrimer composites were also immobilized on Vulcan carbon for XAS. The XAS analysis requires a higher surface concentration of the Pt-dendrimer composites, however, so 2.0 mg of Vulcan carbon per mL of the undiluted (2.0 μM) composite was used. The carbon-supported Pt-dendrimer composites were then filtered using an Advantec PTFE membrane filter (0.5 μm pore size). The filtrate was rinsed with water and then isopropyl alcohol, and allowed to dry in air overnight. The dried powder was pressed into a pellet at 1 ton of pressure for XAS analysis. XAS analysis was performed at the National Synchrotron Light Source at Brookhaven National Lab using beamline X18B. The data were collected in transmission mode using gas ionization detector chambers. A Pt foil was fit to obtain the amplitude reduction factor (S_0^2 = 0.87 for the Pt L_3 edge was used). The data were analyzed using the IFFEFIT and Horae software packages.[26−28] The first shell was fit in R-space using a k-weight of 2 for the Fourier transforms.

Analysis by X-ray Photoelectron Spectroscopy (XPS). A portion of the same pellet used for the XAS analysis was used for XPS. The pellet fragment was dissolved in water, and an aliquot was pipetted onto a chip of glassy carbon. XPS was performed using a Kratos Axis Ultra spectrometer (Chestnut Ridge, NY) having an Al Kα source. Individual elemental spectra were collected with a 0.1 eV step size and a band-pass energy of 20 eV. Binding energies were calibrated against the C 1s line at 284.5 eV.[29] CasaXPS (v 2.3.15, Casa Software, Teignmouth, UK) was used for peak fitting, assuming a mixed Gaussian/Lorentzian model.

RESULTS AND DISCUSSION

Synthesis of Pt DENs by Chemical Reduction. Before describing our new method for complete reduction of Pt DENs, we discuss the original BH_4^--reduction method, which leads to only partial reduction, for comparison. The UV−vis spectra of the G6-OH$(Pt^{2+})_n$ (n = 55, 140, and 225) precursor before and after reduction with BH_4^- are provided in Figure 1. These spectra show that even after reduction with 50-fold excess BH_4^-, a fraction of the ligand-to-metal charge-transfer (LMCT) band of G6-OH$(Pt^{2+})_n$ (λ_{max} = 250 nm) and the absorbance

dx.doi.org/10.1021/la503956h | Langmuir 2014, 30, 15009−15015

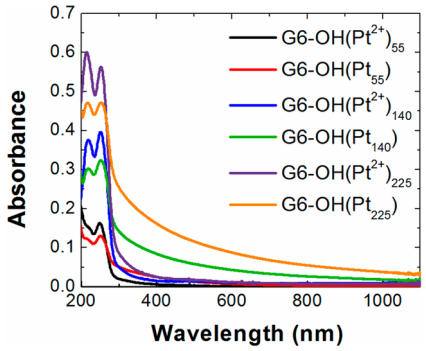

Figure 1. UV−vis spectra of Pt-dendrimer complexes, G6-OH$(Pt^{2+})_n$, and Pt DENs synthesized by BH_4^- reduction, G6-OH(Pt_n), where n = 55, 140, and 225. The spectra were acquired using a 2.0 mm quartz cuvette and blanked with 2.0 μM G6-OH.

bands arising from the unreduced Pt^{2+} salt (λ_{max} = 215 and 230 nm) are present. Consistent with previous findings, this indicates incomplete reduction of the G6-OH$(Pt^{2+})_n$ precursor.[17]

Synthesis of Pt DENs by Galvanic Exchange. As discussed in the Experimental Section, Pt DENs prepared by galvanic exchange are synthesized by sequentially complexing and reducing aliquots of Cu^{2+} in the presence of G6-OH, and then reacting the resulting Cu DENs with Pt^{2+}. To prepare Cu DENs containing more than 64 atoms, multiple complexation and reduction steps are required. This is because, as we have previously shown, the maximum number of Cu^{2+} ions that can be complexed with the interior tertiary amines of G6-OH is 64.[25] Accordingly, the Cu DEN synthesis begins by complexing a slightly substoichiometric amount of Cu^{2+} (55 equiv) with G6-OH. As shown in Figure 2a, this results in a well-defined LMCT band at λ_{max} = 300 nm corresponding to the G6-OH$(Cu^{2+})_{55}$ precursor. Following reduction with BH_4^-, this LMCT band disappears and the characteristic broad absorbance of 55-atom Cu DENs is observed in Figure 2b.[25] After removal of excess BH_4^- by addition of $HClO_4$, 55 additional equiv of Cu^{2+} are added to the solution and the LMCT band is observed again (Figure 2a), but now it is superimposed on the spectrum of the reduced G6-OH(Cu_{55}) DENs. Importantly, the appearance of the LMCT band confirms that no active BH_4^- is present in solution, because the added Cu^{2+} is still in its oxidized form and able to complex to the dendrimer (at pH > 6.5). After the second aliquot of Cu^{2+} is sequestered inside the dendrimer, additional BH_4^- is added to yield reduced DENs containing an average of 110 atoms: G6-OH(Cu_{110}). As shown in Figure 2b this results in an increase in the featureless absorbance spanning the indicated wavelength range. This process is then continued until Cu DENs of the desired size are formed. In this case, we stopped the process at 140 total equiv of Cu in order to make a direct comparison to BH_4^--reduced Pt DENs of the same nominal size (140 is a complete-shell magic number for a truncated octahedron nanoparticle).

The Cu DENs are converted into Pt DENs by adding the same number of equiv of $PtCl_4^{2-}$ as were used to prepare the Cu DENs. As previously reported for the synthesis of G6-OH(Pt_{55}), this galvanic exchange reaction is carried out at pH ~3,[24] with the value here being 3.2. Figure 2c compares UV−vis spectra of the 140-atom Cu DENs at pH > 6.5 and the Pt DENs immediately after galvanic exchange (pH 3.2). Consistent with previous reports, the absorbance of the G6-OH(Pt_{140}) DENs is significantly higher than that of the

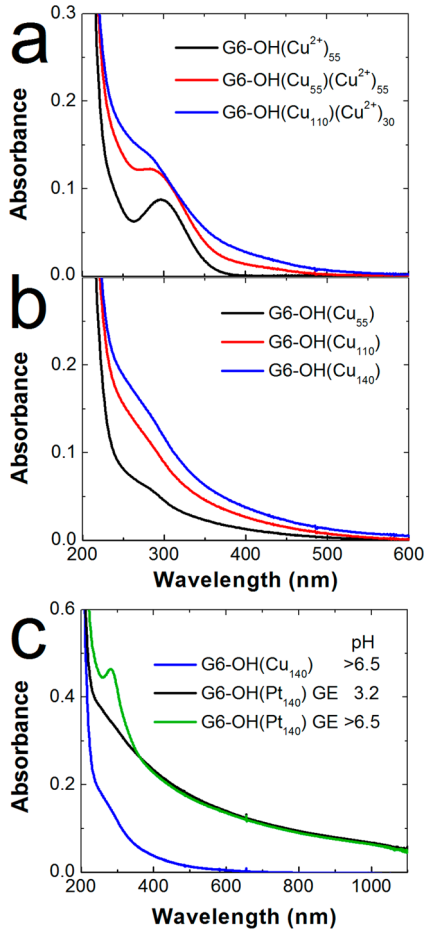

Figure 2. (a) UV−vis spectra for each sequential complexation step of the synthesis of G6-OH(Cu_{140}) DENs. (b) UV−vis spectra for each sequential reduction step in the synthesis of G6-OH(Cu_{140}) DENs. (c) Comparison of the UV−vis spectra of G6-OH(Cu_{140}) prepared by direct reduction with BH_4^- (blue), and G6-OH(Pt_{140}) prepared by galvanic exchange at pH 3.2 (black) and at pH > 6.5 (green). The concentration of the dendrimers in these solutions was 2.0 μM, and the data were obtained using a 2.00 mm quartz cuvette and blanked with water.

corresponding Cu DENs.[24] Additionally, the Cu-LMCT band (λ_{max} = 300 nm) is absent after galvanic exchange at pH 3.2, because the interior tertiary amines of the dendrimer are protonated and hence not available for complexation with Cu^{2+}.[24] For direct comparison with the G6-OH(Cu_{140}) spectrum, the pH of the G6-OH(Pt_{140}) solution was then raised above 6.5. In this case, the pH is high enough that the interior tertiary amines can complex free Cu^{2+}, and a Cu-LMCT band is again apparent. This confirms that galvanic exchange has occurred and that Cu^{2+} is present in the solution.

Pt DENs larger than n = 140 can also be made by galvanic exchange. For example, Figure S1 in the Supporting Information compares G6-OH(Pt_{140}) and G6-OH(Pt_{225}) DENs. The absorbance of G6-OH(Pt_{225}) is higher at all wavelengths, qualitatively indicating the presence of larger nanoparticles.

Following synthesis, the Pt DENs were immobilized on Vulcan carbon, which as we have shown previously is a good support for performing electrocatalytic experiments using DENs.[30,31] Immobilization was carried out at pH 3.2 by the addition of Vulcan carbon and subsequent filtration as

dx.doi.org/10.1021/la503956h | Langmuir 2014, 30, 15009−15015

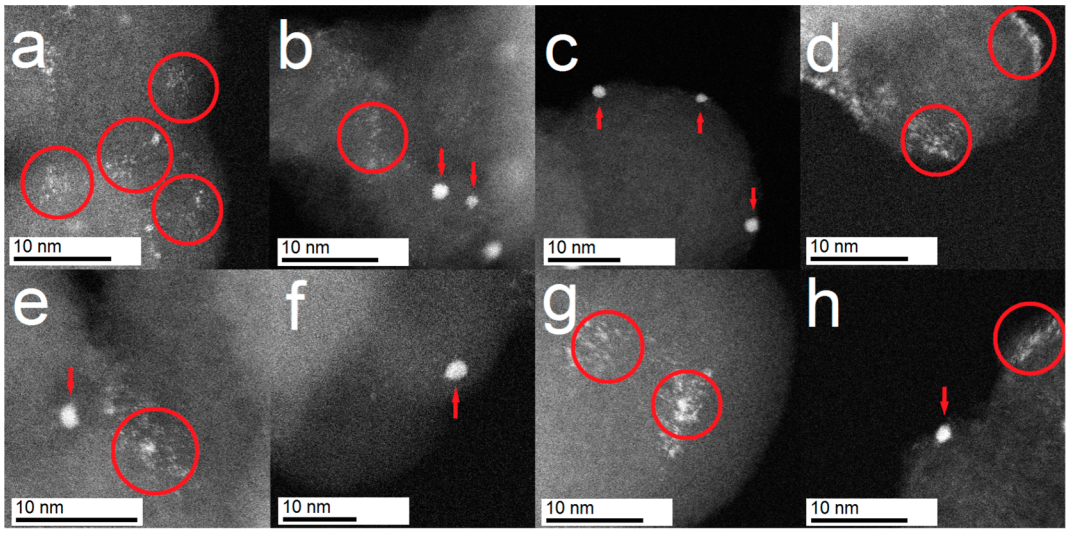

Figure 3. Representative STEM images of (a) the G6-OH$(Pt^{2+})_{55}$ precursor complex, (b) G6-OH(Pt_{55}) synthesized by direct reduction with BH_4^-, (c) G6-OH(Pt_{55}) synthesized by galvanic exchange, (d) the G6-OH$(Pt^{2+})_{140}$ precursor complex, (e) G6-OH(Pt_{140}) synthesized by direct reduction with BH_4^-, (f) G6-OH(Pt_{140}) synthesized by galvanic exchange, (g) the G6-OH$(Pt^{2+})_{225}$ precursor complex, and (h) G6-OH(Pt_{225}) synthesized by direct reduction with BH_4^-. The red circles (~7 nm in diameter) represent the approximate diameter of a G6 PAMAM dendrimer, and they highlight the groupings of ions initially present in the precursor complex or after incomplete reduction of the precursor complex. The red arrows indicate the location of fully reduced DENs.

described in the Experimental Section. TEM images and size-distribution histograms of G6-OH(Pt_{140}) and G6-OH(Pt_{225}) immobilized on Vulcan, prepared using the aforementioned procedure, are shown in Supporting Information Figure S2. Consistent with expectations, these data indicate that the DENs have diameters of 1.7 ± 0.2 nm for G6-OH(Pt_{140}) (calculated diameter =1.6 nm) and 1.9 ± 0.2 nm for G6-OH(Pt_{225}) (calculated diameter = 1.9 nm).[14]

STEM Results. The conclusion that a bimodal distribution of fully reduced and unreduced DENs results from the standard BH_4^-reduction method relies in part on results from a previous TEM study. In that earlier analysis, micrographs showed that direct reduction resulted in Pt DENs having the expected size distribution despite other analytical methods indicating incomplete reduction.[17] At that time, however, we did not have access to electron microscopy with sufficient resolution and contrast to image the G6-OH$(Pt^{2+})_n$ precursor. Now, by utilizing high-resolution aberration-corrected STEM, individual Pt atoms/ions are visible, and hence it is possible to distinguish between the G6-OH$(Pt^{2+})_n$ precursor and G6-OH(Pt_n) DENs. The STEM data discussed next confirm that BH_4^- reduction results in a bimodal distribution of reduced and unreduced DENs.

Figure 3a is a STEM micrograph of the G6-OH$(Pt^{2+})_{55}$ precursor that has not been exposed to BH_4^-. This image shows clusters of individual Pt atoms/ions on the Vulcan carbon surface. To highlight the nature of these groupings, red circles having diameters of ~7 nm (the approximate diameter of G6 PAMAM dendrimers)[32] have been overlaid onto the image. Although highly qualitative, it is not difficult to imagine that these clusters of atoms/ions are contained within individual dendrimers. The micrograph in Figure 3b was obtained after direct BH_4^- reduction of the G6-OH$(Pt^{2+})_{55}$ precursor. In this case, both ordered nanoparticles (~1.3 nm,[17] indicated by red arrows) and a grouping of atoms (red circle) are visible on the Vulcan carbon support. This observation is consistent with the partial (bimodal) reduction model. Specifically, the approximate spread of the disordered atoms is maintained at ~7 nm, suggesting that some of the complexes are unaffected by the chemical reduction process.

Figure 3c shows that G6-OH(Pt_{55}) DENs synthesized by galvanic exchange of Cu for Pt reveal no sign of the unreduced G6-OH$(Pt^{2+})_{55}$ complex (that is, no evidence of individual atoms were apparent despite extensive analysis of the grid). Rather, only fully reduced particles were observed. This same trend is observed for G6-OH$(Pt^{2+})_{140}$, G6-OH(Pt_{140}) prepared by BH_4^- reduction, and G6-OH(Pt_{140}) prepared by galvanic exchange (Figure 3d,e,f, respectively) and for G6-OH$(Pt^{2+})_{225}$ and G6-OH(Pt_{225}) prepared by BH_4^- reduction (Figure 3g and h, respectively). In summary, the representative micrographs shown in Figure 3 confirm, qualitatively, our earlier bimodal-distribution model, wherein a fraction of the G6-OH$(Pt^{2+})_n$ species remain unreduced when exposed to BH_4^-, while the remainder are reduced to yield G6-OH(Pt_n) DENs.[17] In contrast, galvanic exchange results in complete reduction. We wish to emphasize, however, that a much larger statistical analysis would be required to confirm these conclusions if they were solely based on electron microscopy. As discussed in the next three sections, however, spectroscopic evidence is conclusive.

XPS Analysis. Although it is difficult to obtain quantitative information about the extent of Pt DEN reduction from TEM studies, XPS is very well suited for this purpose. Accordingly, we used XPS to compare the extent of reduction using the BH_4^- and galvanic exchange approaches. As shown in Figure 4a, the Pt $4f_{7/2}$ peaks for G6-OH$(Pt^{2+})_n$ (n = 55, 140, and 225) are present at 72.9, 73.3, and 73.5 eV, respectively. These values can be compared with that of the $PtCl_4^{2-}$ starting material: 73.4 eV (black vertical line).[29] The slight shift to lower binding energy as the Pt:dendrimer ratio decreases may result from the increased availability of dendrimer binding sites at lower Pt^{2+} concentrations and the corresponding increase in multidentate binding.[19,22]

The spectra of the BH_4^--reduced DENs (G6-OH(Pt_n), n = 55, 140, and 225) exhibit multiple pairs of peaks, which is consistent with partial reduction and two populations of Pt

dx.doi.org/10.1021/la503956h | Langmuir 2014, 30, 15009−15015

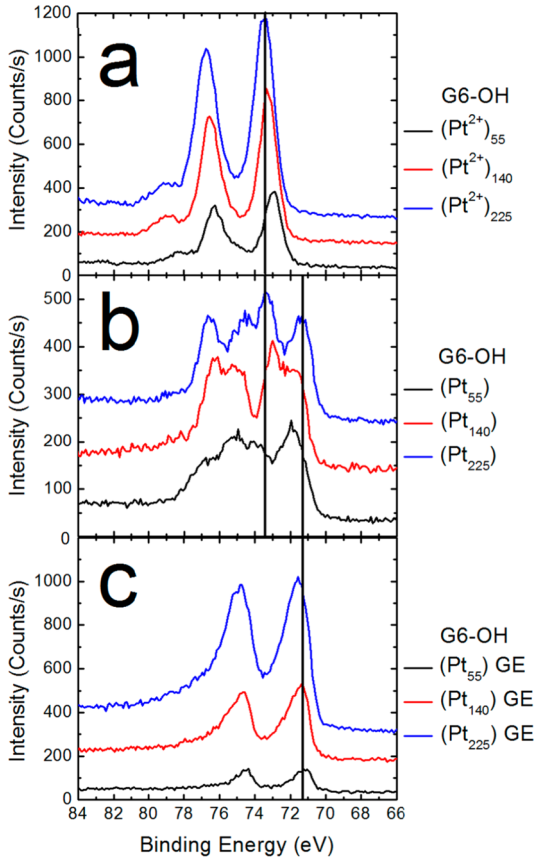

Figure 4. High-resolution XPS spectra of (a) G6-OH(Pt^{2+})$_n$, (b) G6-OH(Pt_n) synthesized by direct reduction with BH_4^-, and (c) G6-OH(Pt_n) synthesized by galvanic exchange (GE), where n = 55, 140, and 225. The vertical black lines at 73.4 and 71.3 eV represent literature values for the binding energies of $PtCl_4^{2-}$ and fully reduced Pt DENs, respectively.

oxidation states. Focusing on the Pt $4f_{7/2}$ region, the peaks at ~71.8 ± 0.2 eV correspond to zerovalent DENs. The black vertical line at 71.3 eV marks the value previously reported for the $4f_{7/2}$ peak for Pt DENs.[17] In addition to these zerovalent Pt 4f peaks, a second set of 4f peaks, corresponding to the G6-OH(Pt^{2+})$_n$ precursor, are also present. These results are consistent with our previous finding that the BH_4^- method leads to only partial reduction of the precursor.[17]

The XPS peaks in Figure 4b were fit to quantify the extent of reduction for each sample. The fits are shown in Supporting Information Figure S3 and quantitative results are provided in Table 1. In all cases, the total XPS spectra are well represented by deconvolution into peaks corresponding to the Pt^0 and Pt^{2+} binding energies. The extent of reduction determined from these fits is 59%, 40%, and 43% for G6-OH(Pt_n) (n = 55, 140, and 225) DENs, respectively. These values are somewhat different than those we have reported previously for n = 55, 147, and 240: 14%, 44%, and 64%, respectively.[17] We attribute the large difference in the percent reduction of G6-OH(Pt_{55}) to the larger excess of BH_4^- used for reduction in the present set of experiments (50-fold versus 10-fold).

Table 1. Percentage Reduction of Pt DENs Synthesized by Direct BH_4^- Reduction

	percentage reduction	
	XPS	XANES
G6-OH(Pt_{55})	59%	54%
G6-OH(Pt_{140})	40%	42%
G6-OH(Pt_{225})	43%	50%

Figure 4c shows XPS spectra of the G6-OH(Pt_n) DENs prepared by galvanic exchange. In contrast to the spectra of the BH_4^--reduced DENs in Figure 4b, these spectra exhibit just one $4f_{7/2}$ peak corresponding to fully reduced Pt. These results indicate that complete galvanic exchange has occurred with the Cu DENs and that little or no unreduced Pt salt or complex is present in the sample.

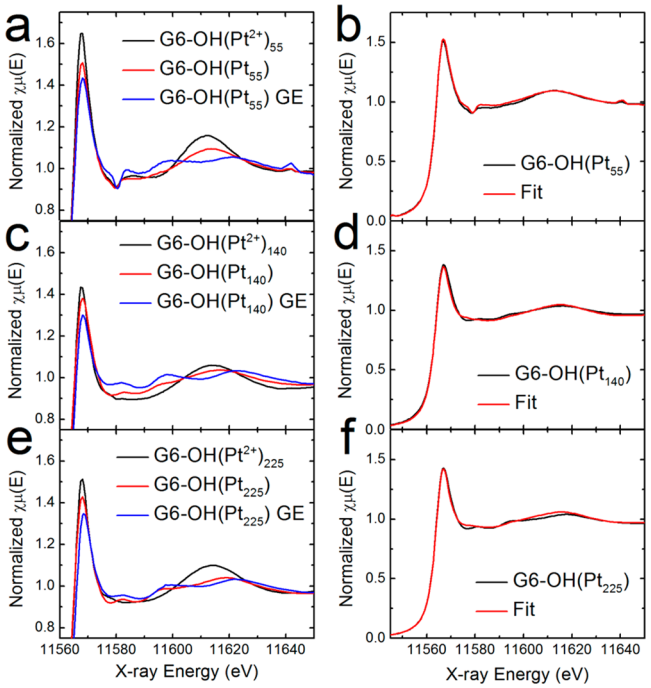

Figure 5. XANES data (left) and LCA fits (right) for (a,b) G6-OH(Pt_{55}), (c,d) G6-OH(Pt_{140}), and (e,f) G6-OH(Pt_{225}). For the right panel, the data corresponding to the DENs synthesized by BH_4^- reduction are shown in black and the LCA best fit is in red.

XANES Analysis. XANES linear combination analysis (LCA) was used to further quantify the extent of Pt reduction and to verify the XPS results. Figure 5a shows that the white line intensity of the G6-OH(Pt_{55}) DENs prepared by direct BH_4^- reduction is between that of the corresponding G6-OH(Pt^{2+})$_{55}$ precursor and G6-OH(Pt_{55}) DENs synthesized by galvanic exchange. The spectrum of G6-OH(Pt_{55}) prepared by direct reduction and the fit obtained from a linear combination of the G6-OH(Pt^{2+})$_{55}$ precursor and G6-OH(Pt_{55}) prepared by galvanic exchange are shown in Figure 5b. The overlap is nearly exact, and it indicates a percentage reduction of the precursor of 59%, which compares favorably with the value of 54% determined by XPS (Table 1).

XANES spectra for the n = 140 and 225 DENs and DEN precursors are shown in Figure 5c and e, respectively. The corresponding LCA fitting for the G6-OH(Pt_{140}) and G6-OH(Pt_{225}) DENs (direct BH_4^- reduction) in Figure 5d and f, respectively, provide good matches. The resulting percentage reductions of the precursors are within 7% of those determined by XPS (Table 1).

EXAFS Analysis. EXAFS spectra were acquired to obtain the coordination number for the fully reduced G6-OH(Pt_n)

dx.doi.org/10.1021/la503956h | Langmuir 2014, 30, 15009−15015

DENs synthesized by galvanic exchange. Figure 6 shows the *R*-space data and corresponding fits. The fits yield coordination numbers of 8.9 ± 1.2 for G6-OH(Pt_{140}) and 9.2 ± 1.2 for G6-OH(Pt_{225}). These values can be compared to those calculated for 140-atom and 225-atom truncated octahedra of 9.09 and 9.49, respectively.[33] These values are substantially higher than those reported previously for Pt DENs reduced with BH_4^-: 3.99 ± 0.61 for G6-OH(Pt_{147}) and 6.09 ± 0.42 for G6-OH(Pt_{240}).[17] The latter very low coordination numbers indicate the presence of a substantial number of unreduced Pt species, which is consistent with the previously discussed XANES and XPS results. An important outcome of the EXAFS analysis is that in the future it will be possible to use in situ electrochemical EXAFS to study electrocatalysis at fully reduced Pt DENs.

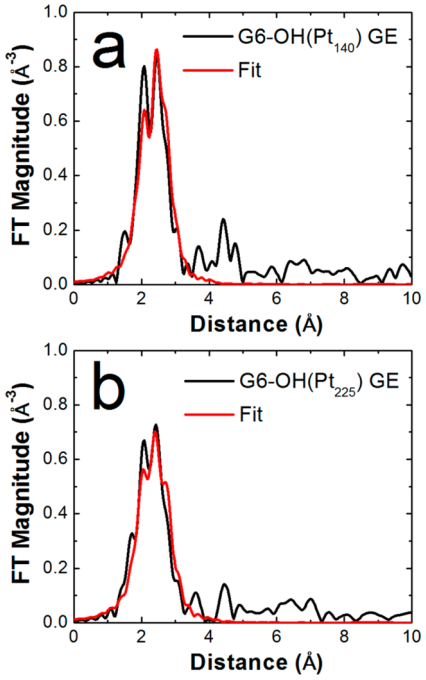

Figure 6. EXAFS data (black) and *R*-space fits (red) (*k*-weight of 2) for Pt DENs prepared by galvanic exchange.

SUMMARY AND CONCLUSIONS

A general scheme for synthesizing fully reduced Pt DENs has been described. The synthesis is carried out by first preparing Cu DENs of the desired size, and then using the process of galvanic exchange to convert these into Pt DENs containing the same number of atoms. We also re-examined the originally reported method for preparing Pt DENs by direct reduction using BH_4^-,[17] and confirmed that this approach leads to a bimodal distribution of fully reduced DENs and fully unreduced precursors.

The present research focus of our group is reconciling the experimentally measured and theoretically calculated electrocatalytic properties of DENs. Due to their high activity for many catalytic reactions, Pt DENs are among the most important materials for developing this type of structure–activity relationship. The types of future studies we envision require, to the maximum extent possible, homogeneity in catalyst size and structure, and the results reported here move us a step closer to this goal.

ASSOCIATED CONTENT

Supporting Information

UV–vis spectra of Pt DENs synthesized by galvanic exchange, TEM images and size-distribution histograms of DENs prepared by galvanic exchange, and deconvolution of XPS spectra. This material is available free of charge via the Internet at http://pubs.acs.org.

AUTHOR INFORMATION

Corresponding Author

*E-mail: crooks@cm.utexas.edu; Phone: 512-475-8674.

Notes

The authors declare no competing financial interest.

ACKNOWLEDGMENTS

We acknowledge support from the Chemical Sciences, Geosciences, and Biosciences Division, Office of Basic Energy Sciences, Office of Science, U. S. Department of Energy (Contract: DE-FG02-13ER16428). R.M.C. thanks the Robert A. Welch Foundation (Grant F-0032) for sustained support. The JEOL JEM-ARM200F STEM was supported by a grant from the National Institute on Minority Health and Health Disparities (G12MD007591). We thank the Surface Analysis Laboratory at the Texas Materials Institute and the National Science Foundation (Grant No. 0618242) for funding the Kratos Axis Ultra XPS used in this work. We are grateful to Dr. Hugo Celio for his assistance with the XPS measurements. Use of the NSLS is supported by the U.S. Department of Energy, Office of Science, Office of Basic Energy Sciences, under Contract No. DE-AC02-98CH10886. Beamline X18B at the NSLS is supported in part by the Synchrotron Catalysis Consortium, U.S. Department of Energy Grant No. DE-FG02-05ER15688.

REFERENCES

(1) Zheng, J.; Petty, J. T.; Dickson, R. M. High Quantum Yield Blue Emission from Water-Soluble Au_8 Nanodots. *J. Am. Chem. Soc.* **2003**, *125*, 7780–7781.

(2) Myers, V. S.; Weir, M. G.; Carino, E. V.; Yancey, D. F.; Pande, S.; Crooks, R. M. Dendrimer-Encapsulated Nanoparticles: New Synthetic and Characterization Methods and Catalytic Applications. *Chem. Sci.* **2011**, *2*, 1632–1646.

(3) Bronstein, L. M.; Shifrina, Z. B. Dendrimers As Encapsulating, Stabilizing, or Directing Agents for Inorganic Nanoparticles. *Chem. Rev.* **2011**, *111*, 5301–5344.

(4) Qian, H.; Zhu, M.; Wu, Z.; Jin, R. Quantum Sized Gold Nanoclusters with Atomic Precision. *Acc. Chem. Res.* **2012**, *45*, 1470–1479.

(5) Cuenya, B. R. Synthesis and Catalytic Properties of Metal Nanoparticles: Size, Shape, Support, Composition, and Oxidation State Effects. *Thin Solid Films* **2010**, *518*, 3127–3150.

(6) Kim, B. H.; Hackett, M. J.; Park, J.; Hyeon, T. Synthesis, Characterization, and Application of Ultrasmall Nanoparticles. *Chem. Mater.* **2014**, *26*, 59–71.

(7) Li, N.; Zhao, P.; Astruc, D. Anisotropic Gold Nanoparticles: Synthesis, Properties, Applications, and Toxicity. *Angew. Chem., Int. Ed.* **2014**, *53*, 1756–1789.

(8) Yancey, D. F.; Chill, S. T.; Zhang, L.; Frenkel, A. I.; Henkelman, G.; Crooks, R. M. A Theoretical and Experimental Examination of Systematic Ligand-Induced Disorder in Au Dendrimer-Encapsulated Nanoparticles. *Chem. Sci.* **2013**, *4*, 2912–2921.

(9) Anderson, R. M.; Zhang, L.; Loussaert, J. A.; Frenkel, A. I.; Henkelman, G.; Crooks, R. M. An Experimental and Theoretical Investigation of the Inversion of Pd@Pt Core@Shell Dendrimer-Encapsulated Nanoparticles. *ACS Nano* **2013**, *7*, 9345–9353.

(10) Zhang, L.; Iyyamperumal, R.; Yancey, D. F.; Crooks, R. M.; Henkelman, G. Design of Pt-Shell Nanoparticles with Alloy Cores for the Oxygen Reduction Reaction. *ACS Nano* **2013**, *7*, 9168−9172.
(11) Zhao, M.; Crooks, R. M. Homogeneous Hydrogenation Catalysis with Monodisperse, Dendrimer-Encapsulated Pd and Pt Nanoparticles. *Angew. Chem., Int. Ed.* **1999**, *38*, 364−366.
(12) Scott, R. W. J.; Datye, A. K.; Crooks, R. M. Bimetallic Palladium−Platinum Dendrimer-Encapsulated Catalysts. *J. Am. Chem. Soc.* **2003**, *125*, 3708−3709.
(13) Lang, H.; May, R. A.; Iversen, B. L.; Chandler, B. D. Dendrimer-Encapsulated Nanoparticle Precursors to Supported Platinum Catalysts. *J. Am. Chem. Soc.* **2003**, *125*, 14832−14836.
(14) Ye, H.; Crooks, J. A.; Crooks, R. M. Effect of Particle Size on the Kinetics of the Electrocatalytic Oxygen Reduction Reaction Catalyzed by Pt Dendrimer-Encapsulated Nanoparticles. *Langmuir* **2007**, *23*, 11901−11906.
(15) Myers, V. S.; Frenkel, A. I.; Crooks, R. M. In Situ Structural Characterization of Platinum Dendrimer-Encapsulated Oxygen Reduction Electrocatalysts. *Langmuir* **2012**, *28*, 1596−1603.
(16) Weir, M. G.; Myers, V. S.; Frenkel, A. I.; Crooks, R. M. In situ X-ray Absorption Analysis of ∼1.8 nm Dendrimer-Encapsulated Pt Nanoparticles during Electrochemical CO Oxidation. *ChemPhysChem* **2010**, *11*, 2942−2950.
(17) Knecht, M. R.; Weir, M. G.; Myers, V. S.; Pyrz, W. D.; Ye, H.; Petkov, V.; Buttrey, D. J.; Frenkel, A. I.; Crooks, R. M. Synthesis and Characterization of Pt Dendrimer-Encapsulated Nanoparticles: Effect of the Template on Nanoparticle Formation. *Chem. Mater.* **2008**, *20*, 5218−5228.
(18) Alexeev, O. S.; Siani, A.; Lafaye, G.; Williams, C. T.; Ploehn, H. J.; Amiridis, M. D. EXAFS Characterization of Dendrimer−Pt Nanocomposites Used for the Preparation of Pt/γ-Al_2O_3 Catalysts. *J. Phys. Chem. B* **2006**, *110*, 24903−24914.
(19) Borodko, Y.; Thompson, C. M.; Huang, W.; Yildiz, H. B.; Frei, H.; Somorjai, G. A. Spectroscopic Study of Platinum and Rhodium Dendrimer (PAMAM G4OH) Compounds: Structure and Stability. *J. Phys. Chem. C* **2011**, *115*, 4757−4767.
(20) Borodko, Y.; Ercius, P.; Pushkarev, V.; Thompson, C.; Somorjai, G. From Single Pt Atoms to Pt Nanocrystals: Photoreduction of Pt^{2+} Inside of a PAMAM Dendrimer. *J. Phys. Chem. Lett.* **2012**, *3*, 236−241.
(21) Ozturk, O.; Black, T. J.; Perrine, K.; Pizzolato, K.; Williams, C. T.; Parsons, F. W.; Ratliff, J. S.; Gao, J.; Murphy, C. J.; Xie, H.; Ploehn, H. J.; Chen, D. A. Thermal Decomposition of Generation-4 Polyamidoamine Dendrimer Films: Decomposition Catalyzed by Dendrimer-Encapsulated Pt Particles. *Langmuir* **2005**, *21*, 3998−4006.
(22) Pellechia, P. J.; Gao, J.; Gu, Y.; Ploehn, H. J.; Murphy, C. J. Platinum Ion Uptake by Dendrimers: An NMR and AFM Study. *Inorg. Chem.* **2004**, *43*, 1421−1428.
(23) Zhao, M.; Crooks, R. M. Intradendrimer Exchange of Metal Nanoparticles. *Chem. Mater.* **1999**, *11*, 3379−3385.
(24) Pande, S.; Weir, M. G.; Zaccheo, B. A.; Crooks, R. M. Synthesis, Characterization, and Electrocatalysis using Pt and Pd Dendrimer-Encapsulated Nanoparticles Prepared by Galvanic Exchange. *New J. Chem.* **2011**, *35*, 2054−2060.
(25) Zhao, M.; Sun, L.; Crooks, R. M. Preparation of Cu Nanoclusters within Dendrimer Templates. *J. Am. Chem. Soc.* **1998**, *120*, 4877−4878.
(26) Newville, M. IFEFFIT: Interactive XAFS Analysis and FEFF Fitting. *J. Synchrotron Radiat.* **2001**, *8*, 322−324.
(27) Ravel, B.; Newville, M. ATHENA, ARTEMIS, HEPHAESTUS: Data Analysis for X-ray Absorption Spectroscopy Using IFEFFIT. *J. Synchrotron Radiat.* **2005**, *12*, 537−541.
(28) Ravel, B. ATOMS: Crystallography for the X-ray Absorption Spectroscopist. *J. Synchrotron Radiat.* **2001**, *8*, 314−316.
(29) *NIST X-ray Photoelectron Spectroscopy Database*, Version 4.1; National Institute of Standards and Technology: Gaithersburg, MD, 2012; http://srdata.nist.gov/xps/.
(30) Yancey, D. F.; Zhang, L.; Crooks, R. M.; Henkelman, G. Au@Pt Dendrimer Encapsulated Nanoparticles As Model Electrocatalysts for Comparison of Experiment and Theory. *Chem. Sci.* **2012**, *3*, 1033−1040.
(31) Iyyamperumal, R.; Zhang, L.; Henkelman, G.; Crooks, R. M. Efficient Electrocatalytic Oxidation of Formic Acid Using Au@Pt Dendrimer-Encapsulated Nanoparticles. *J. Am. Chem. Soc.* **2013**, *135*, 5521−5524.
(32) Jackson, C. L.; Chanzy, H. D.; Booy, F. P.; Drake, B. J.; Tomalia, D. A.; Bauer, B. J.; Amis, E. J. Visualization of Dendrimer Molecules by Transmission Electron Microscopy (TEM): Staining Methods and Cryo-TEM of Vitrified Solutions. *Macromolecules* **1998**, *31*, 6259−6265.
(33) Glasner, D.; Frenkel, A. I. Geometrical Characteristics of Regular Polyhedra: Application to EXAFS Studies of Nanoclusters. *AIP Conf. Proc.* **2007**, *882*, 746−748.